JOURNAL OF SOLID STATE CHEMISTRY **132,** 24–32 (1997)
ARTICLE NO. SC977396

Antiferromagnetic Coupling in the Cyclic Octanuclear Compound [Cu(II)(μ-3,5-dimethylpyrazolate)(μ-OH)] and Its Analogue [Cu(II)(μ-pyrazolate)(μ-OH)]

Rodolfo Acevedo-Chávez,* María Eugenia Costas,†,[1] and Roberto Escudero‡

*Centro de Química, Instituto de Ciencias, B. Universidad Autónoma de Puebla, Apartado Postal 1613, Puebla, Puebla, México; †Facultad de Química, Universidad Nacional Autónoma de México, 04510 México, D.F., México; and ‡Instituto de Investigaciones en Materiales, Universidad Nacional Autónoma de México, 04510 México, D.F., México

Received July 1, 1996; in revised form January 16, 1997; accepted March 19, 1997

The spectral and magnetic characterization of the cyclic octanuclear compound [Cu(II)$_8$(μ-3,5-dimethylpyrazolate)$_8$(μ-OH)$_8$] and its analogue [Cu(II)(μ-pyrazolate)(μ-OH)] are reported. An octanuclear ring magnetic model describes the magnetic data of the first compound, in agreement with a strong antiferromagnetic coupling between the Cu(II) centers through the mixed bridging ligands. The same results are obtained for its Cu(II) analogue, which let us consider the existence of a structural arrangement of the same type for [Cu(II)(μ-pyrazolate)(μ-OH)].

INTRODUCTION

As part of a methodology in the coordination chemistry study of the family of the purinic derivatives, their structural analogues, and their isomers, selective heterocyclic fragments serve as models of certain regions of the whole original molecules. For example, by selecting the heterocycle pyrazole and derivatives, it is possible to study some aspects of the coordination chemistry of the purinic isomer allopurinol in a simpler way. We have been interested in the coordination chemistry of the pyrazolic fragment of allopurinol; we have selected the pyrazole (1) and 3,5-dimethylpyrazole heterocycles (2) (Fig. 1) to explore their interactions with metallic atoms (e.g., Cu(II)) under several reaction conditions systematically modified and to analyze the structural, spectral, and magnetic properties of the respective coordination compounds.

In the progress of our research program the synthesis and structural characterization of the cyclic octanuclear coordination compound [Cu(II)$_8$(μ-3,5-dimethylpyrazolate)$_8$(μ-OH)$_8$] were reported (3, 4). In these papers the formation of the polynuclear compound [Cu(II)(μ-pyrazolate)(μ-OH)] was also mentioned. However, no detailed information about the synthesis conditions and physical properties was given for the last Cu(II) compound. These aspects prompted us to explore the syntheses for these two coordination compounds (both by the reported and by alternative routes) to perform their spectral and magnetic characterization, and to compare their physical properties with those shown by the related polynuclear compound [Cu(II)(μ-allopurinolate)(μ-OH)] reported before (5).

The magnetic study reported here represents the first analysis ever done of these interesting systems, in which the pyrazolic ligands and OH groups simultaneously bridge the Cu(II) centers.

EXPERIMENTAL

1. Materials. 1*H*-pyrazole (pzH), 1*H*-3,5-dimethylpyrazole (3,5-dmpzH), and the metallic Cu(II) salts (analytical grade) were commercially supplied. There was no need for further purification.

2. Synthesis. The polynuclear compound [Cu(II)(μ-pz)(μ-OH)] was prepared by dissolving 1 mmol of pzH in ca. 50 ml of an aqueous buffer solution at pH 13 (KCl/NaOH) upon stirring at room temperature. The respective Cu(II) metallic salt ($X = Cl^-$, Br^-, NO_3^-, SO_4^{2-}, or ClO_4^-) (1 mmol), previously dissolved in ca. 10 ml of H_2O, was added to the colorless solution previously obtained. The resulting deep blue suspension of each reaction was maintained under stirring at room temperature. All of them changed to a blue–purple color in a few hours. The corresponding reaction mixture was kept under these conditions for ca. 24 h with no observed changes. The suspension was filtered off and the solid product (blue–purple color) was washed first with several portions of H_2O and then with repetitive volumes of C_2H_5OH. When kept at ca. 100°C for

[1] To whom correspondence should be addressed.

0022-4596/97 $25.00

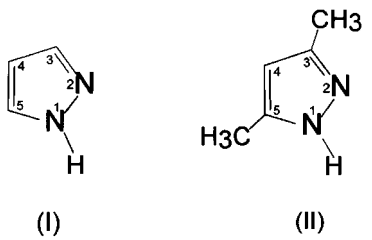

FIG. 1. Schematic drawing of 1*H*-pyrazole (I) and 1*H*-3,5-dimethylpyrazole (II).

4 h, each solid showed no changes. The respective colorless filtrate was discarded. When $X = CH_3CO_2^-$ was used as the metallic counterion, the deep blue suspension (under stirring for ca. 48 h) changed to a blue–purple suspension, and when it was kept under the same conditions for an additional 48 h, no changes were detected. The reaction mixture and the solid product were treated as above.

Deep purple–black solids were obtained by carrying out the same reactions at boiling temperature (except for $X = SO_4^{2-}$). These solids correspond to mixtures of CuO and $Cu(II)_n(pz)_n(OH)_{n/2}(X)_{n/2}$ in a ratio directly proportional to the reaction time.

The synthesis of $[Cu(II)_8(\mu\text{-dmpz})_8(\mu\text{-OH})_8]$ required the previous preparation of CuI and its reaction with 3,5-dmpzH, giving the starting cyclic trinuclear Cu(I) coordination compound $[Cu(I)_3(\mu\text{-3,5-dmpz})_3]$. This reaction was performed as follows: 10.0 mmol of CuI was dissolved in 80 ml of CH_3CN under stirring at room temperature and N_2(g) atmosphere (the solvent was previously bubbled with N_2(g)). Sheets of Cu(s) were added to the resulting solution (pale yellow). First 10.0 mmol of 3,5-dmpzH and then 11.0 mmol of $(C_2H_5)_3N$ were incorporated to the reaction mixture, rapidly forming a white suspension, which was maintained under stirring at room temperature and N_2(g) for half an hour. The mixture was filtered off. A white solid was isolated and washed first with 50 ml of CH_3CN and then with 50 ml of $(CH_3)_2CO$. The solid product was kept at 105°C for half an hour, and no changes were observed. The product was found to be insoluble in the common organic solvents, and stable in air and moisture. The IR bands of the product were the same as those quoted for the Cu(I) compound in a crystalline structure determination (6), in which another synthetic method was used. Finally, the cyclic trinuclear compound $[Cu(I)_3(\mu\text{-dmpz})_3]$ was employed in the synthesis of $[Cu(II)_8(\mu\text{-dmpz})_8(\mu\text{-OH})_8]$, with a very similar technique to that previously reported (4), as follows: 0.98 g of $[Cu(I)_3(\mu\text{-dmpz})_3]$ was added to 40 ml of C_5H_5N with 0.5 ml of deionized H_2O. A vigorous stream of O_2(g) was applied to the reaction mixture under stirring at room temperature. A slow change to deep blue color was observed; no changes were detected in the next 24 h. The suspension was filtered off, and a deep blue–purple solid was isolated and washed with ca. 20 ml of C_5H_5N. The product was dried at reduced pressure and room temperature. The original filtrate and the C_5H_5N used in the washing were mixed and evaporated to dryness, getting a second fraction of the same product.

3. Physical measurements. Infrared (IR) spectra (Nujol mulls, KBr windows) in the 4000–400 cm^{-1} range were obtained by using a 750 FT IR Nicolet equipment. For the 4000–200 cm^{-1} range (Nujol mulls, CsI windows) a 598 Perkin–Elmer spectrometer was employed. IR data (high density polyethylene pellets) in the 600–70 cm^{-1} range were obtained by using a 740 FT IR Nicolet equipment.

Electronic spectra (200–1100 nm, quartz windows and $BaSO_4$ as reference) in the solid state of the powdered samples were recorded using a 160-A Shimadzu spectrometer.

Thermogravimetric data (room temperature–800°C) were obtained by using a 2100 Dupont thermobalance, employing N_2(g) as carrier gas and 5°C min^{-1} as the heating rate.

X-ray diffraction patterns of the powdered samples were recorded by using a D-500 Siemens diffractometer by employing a secondary monochromator with Cu$K\alpha$ radiation.

X-band EPR spectra of the powdered samples (room temperature and 77 K) were recorded by employing a 200-D Bruker spectrometer, using DPPH as reference.

The magnetic susceptibility of powdered samples as a function of temperature at different magnetic fields was measured with a SQUID Quantum Design magnetometer, from 2 to 300 K and magnetic fields of 100, 1000, and 10000 G. The magnetic susceptibility data were corrected by the cell and the sample diamagnetic contributions. The magnetometer was previously calibrated with very fine standards (Pd, Ni, and Al), and the mean standard deviation of the magnetic susceptibility measurements was three orders of magnitude lower than the studied data. Preliminary magnetic susceptibilities (room temperature) of powdered samples were obtained by using a Johnson Matthey balance and employing Hg $[Co(SCN)_4]$ as reference.

Microanalysis confirmation (C, H, N) was performed at the Chemistry Department, University College of London.

RESULTS AND DISCUSSION

$[Cu(II)(\mu\text{-}pz)(\mu\text{-}OH)]$

1. Analytical results. Experimental, 24.4 (%C), 2.76 (%H), 18.91 (%N); calculated for Cu(II) $(C_3H_3N_2^-)$ (OH^-), 24.4 (%C), 2.73 (%H), 18.98 (%N). These analytical results correspond to the product obtained when $X = SO_4^{2-}$ was employed as the initial Cu(II) metallic counterion, and they are in full agreement with the anionic character of the pyrazolate ligand.

TABLE 1
IR Data (4000–200 cm^{-1}) and Assignments for pzH and [Cu(II)(μ-pz)(μ-OH)]

pzH		[Cu(II)(μ-pz)(μ-OH)]	
$\bar{\nu}$ (cm^{-1})	Assignments	$\bar{\nu}$ (cm^{-1})	Assignments
—	—	3580 M, b 3410 S, b	ν_{OH^-} bridge
3050 S, vb	ν_{N-H} ν_{C-H}	3100 W, b	ν_{N-H} ν_{C-H}
1460 M, b	ν_{ring} ω β_{N-H}	1480 M, s	ν_{ring} ω β_{N-H}
1400 S, s	ν_{ring} ω β_{N-H}	1410 S, b	ν_{ring} ω β_{N-H}
1360 S, d	ν_{ring} ω β_{N-H}	1370 S, s	ν_{ring} ω β_{N-H}
1265 W, d	ring β_{C-H} δ_{C-H} β_{N-H}	1270 S, s	ring β_{C-H} δ_{C-H} β_{N-H}
1235 W, d	β_{C-H} δ_{C-H} β_{N-H} ring	1250 Sh	δ_{C-H} β_{C-H} ring β_{N-H}
1145 S, d	β_{C-H} δ_{N-H} β_{N-H} ring	1170 S, s	β_{C-H} ring δ_{N-H} β_{N-H}
1045 S, d	β_{C-H} δ_{C-H}	1055 S, b	β_{C-H} δ_{C-H}
935 M, b	β_{C-H} δ_{ring}	915 M, b	β_{C-H} δ_{ring}
880 M, b	γ_{C-H} γ_{N-H} δ_{C-H}	865 M, b	γ_{C-H} δ_{C-H} γ_{N-H}
835 M, b	γ_{C-H} γ_{N-H} δ_{C-H}	—	—
760 S, b	γ_{C-H} γ_{N-H} δ_{C-H}	745 S, s	γ_{C-H} γ_{N-H} δ_{C-H}
655 M, s	ring γ_{N-H}	—	—
615 S, d	ring δ_{N-H} γ_{N-H}	615 S, s	ring δ_{N-H} γ_{N-H}
—	—	535 M, b	ν_{M-OH^-} bridge
—	—	465 Sh	ν_{M-OH^-} bridge
—	—	330 S, s	ν_{M-N}

Note. S, strong, M, medium; W, weak; Sh, shoulder; vb, very broad; b, broad; s, sharp; d, doublet.

2. Infrared spectrum. The IR spectral data of several samples of the Cu(II) compound and those corresponding to the free heterocyclic ligand are listed in Table 1. The assignments were made based on recent studies (7–11).

The overall spectral behavior is in agreement with the existence of the pyrazolate as a bridging ligand to Cu(II) centers through the N atoms (7–11). The heterocyclic ligand coordination is supported by a strong and sharp band at 330 cm^{-1}, assigned to the $\nu(M–N)$ vibrational mode. The IR data for the OH group indicate its existence as a bridging ligand (12–15).

With regard to the geometrical disposition of the pyrazolate and OH ligands in the Cu(II) coordination sphere, the low-energy IR data are in agreement with a mutually *trans* configuration, as schematically shown in Fig. 2.

3. Electronic spectrum. The spectra of the samples in the 400–1100 nm range show a broad and asymmetric band centered at 590 nm. The frequency and structure of this band is associated with *d–d* transitions of Cu(II) in a nearly planar tetracoordinated geometry.

4. X-ray diffraction pattern. The powder patterns consist of broad signals in the 7.00–50.00 2θ range. This could be suggestive of a poor crystallinity of all the samples analyzed, associated to the synthesis experimental conditions under which the Cu(II) compound was obtained.

5. EPR spectrum. The X-band ($\nu = 9.79$ GHz) EPR spectra at room temperature of all the samples show a very weak, broad, and symmetric signal with $g_{av} \simeq 2.14$. These spectra are not resolved when the temperature is decreased (77 K). The pattern is associated to the existence of strong Cu(II)–Cu(II) magnetic coupling.

6. Thermogravimetric results. The thermal results do not show mass loss in the room temperature–200°C range.

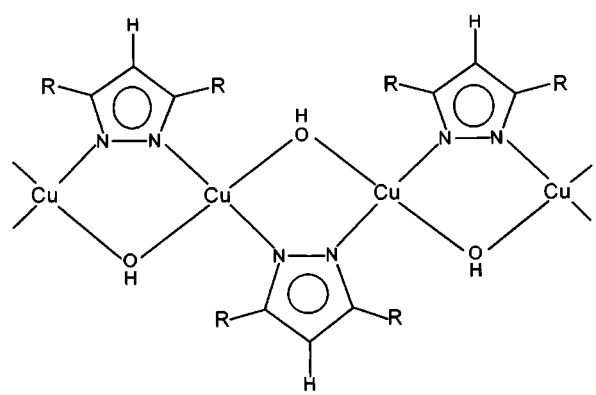

FIG. 2. Schematic drawing of the structural arrangement suggested for [Cu(II)(μ-pz)(μ-OH)] (R = H), and partial drawing of the structural arrangement shown by the octanuclear ring [$Cu(II)_8$(μ-dmpz)$_8$(μ-$OH)_8$] ($R = CH_3$) (References 3 and 4).

This suggests the absence of H_2O molecules both in the lattice and in the metallic coordination sphere. The lowering of mass starts at 232°C (98.88% of initial mass) in an abrupt step; then a second step is observed starting at ca. 237°C (71.39%), and finally a mass loss in steps from ca. 341°C (44.12%) up to 800°C (23.64%) is obtained. The same results were observed when the samples were in contact with ambient air, confirming the nonhygroscopic character of the coordination compound.

7. Preliminary magnetic results. The effective magnetic moment (μ_{eff}) of samples coming from the several reaction conditions ($X = Cl^-$, SO_4^{2-}, ClO_4^-, and $CH_3CO_2^-$) was obtained at room temperature, ranging from 0.94 to 1.0 μ_B/Cu(II) center. The values close to 1.0 μ_B allow us to suggest the existence of a noticeable Cu(II)–Cu(II) magnetic coupling, in agreement with the EPR spectral information.

$[Cu(II)_8(\mu\text{-}dmpz)_8(\mu\text{-}OH)_8]$

1. Infrared spectrum. The IR spectrum of $[Cu(II)_8(\mu\text{-}dmpz)_8(\mu\text{-}OH)_8]$ shows a similar pattern with respect to the IR bands of 3,5-dmpz bonded as the bridging ligand in the cyclic trinuclear system $[Cu(I)_3(\mu\text{-}3,5\text{-}dmpz)_3]$. Table 2 shows the IR bands of the compound under discussion and tentative assignments to them.

The IR spectrum of the coordinated heterocycle shows several modifications when compared to the spectrum of the free ligand. The analysis supports the nonexistence of the N–H group in the heterocyclic ligand. The same analysis gives rise to the existence of perturbations of the bands associated with endocyclic groups vibrational modes in agreement with the participation of the N atoms in their coordination to the Cu(II) centers, and the heterocycle as the bridging ligand. The bands appearing at 371 and 320 cm^{-1} are assigned to $\nu(M\text{–}N)$. The IR spectrum also shows bands associated with the $\nu(OH^-)$ and the $\nu(M\text{–}OH^-$ bridge) vibrational modes, also in concordance with the structural information reported for this Cu(II) compound.

TABLE 2
IR Data (4000–200 cm^{-1}) and Assignments for $[Cu(II)_8(\mu\text{-dmpz})_8(\mu\text{-OH})_8]$

$\bar{\nu}(cm^{-1})$	Assignments
ca. 3400 M, b	ν_{OH^-} bridge
ca. 3100 M,b	—
2900 W, s	ν_{C-H}
1538 S, s	ν_{ring}
1418 S, b	ν_{ring}
1340 S, s	ν_{ring}
1140 W, b	ν_{ring} / β_{C-H}
1040 M, s	δ_{C-H}/β_{C-H}
890 M, b	γ_{C-H} / δ_{C-H}
770 M, s	γ_{C-H} / δ_{C-H}
700 W, s	—
485 M, b	ν_{M-OH^-} bridge
460 M, b	ν_{M-OH^-} bridge
371 M, b	ν_{M-N}
320 W, b	ν_{M-N}

Note. Abbreviations are the same as in Table 1. Assignments were made using the references cited in the discussion of [Cu(II)(μ-pz)(μ-OH)].

2. Electronic spectrum. In the 400–1100 nm range $[Cu(II)_8(\mu\text{-}3,5\text{-}dmpz)_8(\mu\text{-}OH)_8]$ shows a broad band with a maximum at 580 nm, which can be associated to *d–d* transitions of Cu(II) in a roughly planar tetracoordinated Cu(II) geometry. The structure and frequency of this band is similar to that shown by the analogue [Cu(II) (μ-pz) (μ-OH)] (590 nm) and it is in agreement with the Cu(II) $(N)_2(O)_2$ character for both systems.

3. EPR spectrum. At room temperature and $\nu = 9.7$ GHz, $[Cu(II)_8(\mu\text{-}3,5\text{-}dmpz)_8(\mu\text{-}OH)_8]$ is nearly EPR silent. This behavior also indicates remarkable magnetic coupling, as in [Cu(II) (μ-pz) (μ-OH)] under the same spectral conditions. The EPR spectrum was not resolved upon a temperature decrease (77 K).

4. X-ray diffraction pattern. The analyzed samples of the cyclic octanuclear compound $[Cu(II)_8(\mu\text{-}3,5\text{-}dmpz)_8(\mu\text{-}OH_8)]$ show a powder pattern that resembles in some aspects that of the analogue [Cu(II) (μ-pz) (μ-OH)]. The former shows, however, signals of sharper and higher intensity character in the 4–30 2θ range. The differences between the two patterns could be attributed in part to the drastic synthesis conditions carried out. Also, the detailed structural and lattice characteristics of both Cu(II) systems are not necessarily the same, and this may also explain the differences.

5. Thermogravimetric results. $[Cu(II)_8(\mu\text{-}3,5\text{-}dmpz)_8(\mu\text{-}OH)_8]$ shows a different thermogravimetric pattern compared to that shown by its analogue [Cu(II) (μ-pz) (μ-OH)]. It shows a first step of mass loss starting at 86.6°C (98.21% of initial mass). The second step starts at 211.6°C (83.2%) and continues in steps from ca. 334°C (44.34%) up to 800°C (23.21%). The thermal results for the first mass loss step could be associated with the elimination of C_5H_5N solvent molecules from the sample, related to the dryness conditions carried out for this compound synthesis (in fact, in the synthetic route previously reported (4), two C_5H_5N molecules per octanuclear unit were deduced from the analytical results).

6. Preliminary magnetic results. $[Cu(II)_8(\mu\text{-}3,5\text{-}dmpz)_8(\mu\text{-}OH)_8]$ shows an effective magnetic moment at room

temperature of ca. 0.7 μ_B/Cu(II) center. This low value indicates a strong magnetic coupling between the unpaired electrons of the Cu(II) centers, in agreement with the EPR spectrum. This behavior is similar to that deduced for the analogue polynuclear compound [Cu(II)(μ-pz)(μ-OH)].

MAGNETIC STUDIES

The magnetic susceptibility versus temperature measurements were carried out in the 2–300 K range at magnetic fields of 100, 1000, and 10000 G for both compounds.

Figure 3 shows the molar magnetic susceptibility $\bar{\chi}$ (per octanuclear unit) for [Cu(II)(μ-pz)(μ-OH)], as a function of temperature for the three values of the external magnetic field.

The small but continued increase in the $\bar{\chi}$ values with temperature in the high-temperature region indicates an antiferromagnetic coupling. In the low-temperature region, a Curie–Weiss behavior, which may be associated with noncoupled $S = 1/2$ spins, is observed. As the magnetic field increases, a small decrease in the $\bar{\chi}$ values is observed, with no modification in the general trend of the magnetic response. The antiferromagnetic coupling is also inferred from the $\bar{\chi}T$–T plots for the same magnetic fields: a nearly linear decrease in $\bar{\chi}T$ with the temperature decrease is observed. In this representation the three lines for the different H values converge in the limit of low temperature, and the increase of the magnetic field produces a decrease in the respective slopes. Linear relationships that converge at 100 G are obtained when plotting the experimental magnetization data (M) as a function of the magnetic field (H) for the fixed temperatures 10, 70, 200, and 300 K. The line for $T = 10$ K shows a higher slope than that of the others; the slopes for the other three temperatures are very similar, slightly increasing from 70 to 300 K. This behavior corroborates both the noncoupled $S = 1/2$ spins contribution in the low-temperature region and the successive population of excited states of higher spin multiplicity for the high-temperature region, which indicates the existence of magnetic coupling in the solid product.

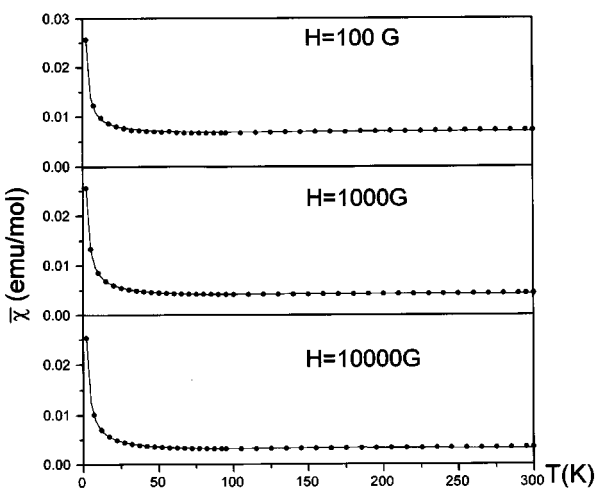

FIG. 3. Molar magnetic susceptibility $\bar{\chi}$ (per octanuclear unit) as a function of temperature and magnetic field for [Cu(II)(μ-pz)(μ-OH)]. Dotted lines are the experimental data and solid lines are theoretical values.

The data were studied employing several magnetic models like the dinuclear, the infinite linear chain, and the finite size ring (i.e., octanuclear). The best fitting results were obtained for the octanuclear ring model of $S = 1/2$ coupled spins (16), for which the parallel magnetic susceptibility expression, modified to take into account the fraction of noncoupled spins (ρ) and the temperature independent term ($\bar{\chi}_0$) contributions, is

$$\bar{\chi} = \frac{N\beta^2 g^2}{4kT}\, e^{-|J|/kT}\left[\frac{1-(-\tanh K)^N}{1+(-\tanh K)^N}\right](1-\rho) + \bar{\chi}_0(1-\rho) + \frac{N\beta^2 g^2}{2kT}\,\rho, \qquad [1]$$

where $K = |J|/2kT$, N is the size of the finite ring (we used $N = 8$), and the other symbols have their usual meaning. In the fitting process, the minimization function used was

$$\sigma^2 = \sum_{i=1}^{N} \frac{(\bar{\chi}_{\text{theor}} - \bar{\chi}_{\text{exp}})^2}{N-n}.$$

The fitting process (employing Eq. [1]) was very successful and gave the following magnetic parameters for $g = 2.14$: $H = 100$ G, $J = -178.6 \pm 4.28$ cm^{-1}, $\rho = 0.045 \pm 1.77 \times 10^{-4}$, $\bar{\chi}_0 = 0.0066 \pm 1.72 \times 10^{-5}$ emu/octanuclear unit; $H = 1000$ G, $J = -226.7 \pm 20.97$ cm^{-1}, $\rho = 0.051 \pm 4.24 \times 10^{-4}$, $\bar{\chi}_0 = 0.0039 \pm 4.85 \times 10^{-5}$ emu/octanuclear unit; $H = 10{,}000$ G, $J = -218.4 \pm 21.47$ cm^{-1}, $\rho = 0.053 \pm 4.73 \times 10^{-4}$, $\bar{\chi}_0 = 0.0029 \pm 5.36 \times 10^{-5}$ emu/octanuclear unit. The J values are consistent with a strong antiferromagnetic coupling between the unpaired electrons of the Cu(II) centers.

The same magnetic model with a mean-field correction was employed to explore the possibility of interring magnetic coupling. The magnetic susceptibility ($\bar{\chi}'$) in this approximation is

$$\bar{\chi}' = \frac{\bar{\chi}}{1-(2zJ'/Ng^2\beta^2)\bar{\chi}}, \qquad [2]$$

where $\bar{\chi}$ is the magnetic susceptibility given by Eq. [1], J' is the interring magnetic coupling parameter, and z is the number of nearest neighboring rings.

From this, a very good fit was obtained for the three fields, with the following magnetic parameters for $g = 2.14$: $H = 100$ G, $J = -191.54 \pm 22.37\ cm^{-1}$, $zJ' = -0.14 \pm 1.38\ cm^{-1}$, $\rho = 0.045 \pm 0.0034$, $\bar{\chi}_0 = 0.0067 \pm 8.73 \times 10^{-5}$ emu/octanuclear unit; $H = 1000$ G, $J = -173.6 \pm 7.97\ cm^{-1}$, $zJ' = -3.73 \pm 0.304\ cm^{-1}$, $\rho = 0.063 \pm 0.001$, $\bar{\chi}_0 = 0.0038 \pm 2.85 \times 10^{-5}$ emu/octanuclear unit; $H = 10{,}000$ G, $J = -167.5 \pm 10.28\ cm^{-1}$, $zJ' = -4.43 \pm 0.41\ cm^{-1}$, $\rho = 0.067 \pm 0.002$, $\bar{\chi}_0 = 0.0027 \pm 4.37 \times 10^{-5}$ emu/octanuclear unit. These parameters correspond to the theoretical curves shown as solid lines in Fig. 3. The J values corroborate a strong antiferromagnetic coupling (intraring type). The zJ' values make us think about the possibility of very weak interring magnetic coupling, maybe of the antiferromagnetic type.

For $[Cu(II)_8(\mu\text{-}3,5\text{-}dmpz)_8(\mu\text{-}OH)_8]$, Fig. 4 shows the molar magnetic susceptibility $\bar{\chi}$ (per octanuclear unit) as a function of temperature for the three magnetic fields.

The general pattern in the high-temperature region also suggests an antiferromagnetic coupling. The behavior in the low-temperature region (Curie–Weiss type) may also be associated with the presence of noncoupled $S = 1/2$ spins. The applied magnetic field leads to a nearly insignificant increase of the $\bar{\chi}$ values, with no changes in the general magnetic response. As in the previous system, the antiferromagnetic coupling is also deduced from the $\bar{\chi}T$–T plots for the three magnetic fields. In this case, and for a magnetic field value, a $\bar{\chi}T$ decrease and a decrease in the slope starting from ca. 130 K are obtained with the temperature decrease. The three curves show the same trend, and they converge at the limit of low temperature. The increase of the magnetic field produces a slight increase in the corresponding slopes.

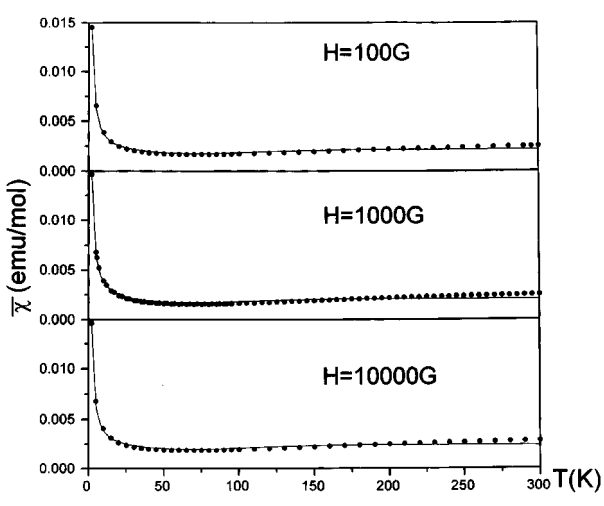

FIG. 4. Molar magnetic susceptibility $\bar{\chi}$ (per octanuclear unit) as a function of temperature and magnetic field for $[Cu(II)_8(\mu\text{-}dmpz)_8(\mu\text{-}OH)_8]$. Dotted lines are experimental data and solid lines are theoretical values.

The M–H plots for the fixed temperatures 10, 70, 200, and 300 K show linear relationships which converge at 100 G. The lines show a progressive increase in slope for 70, 200, 300, and 10 K. These slopes are lower than those found for the previously discussed compound. The slope for 10 K also corroborates the noncoupled $S = 1/2$ spins contribution in the low-temperature region. The increasing slopes for the 70–300 K range are consistent with the population of excited states of higher spin multiplicity. The slopes of the 10 K lines for both Cu(II) compounds allow us to suggest the presence of a higher contribution of noncoupled $S = 1/2$ spins in [Cu(II) (μ-pz) (μ-OH)].

The fitting process was also performed for the model employed before with a mean-field correction (Eq. [2]). In this case, the magnetic parameters obtained for $g = 2.20$ were $H = 100$ G, $J = -173.0 \pm 14.5\ cm^{-1}$, $zJ' = +7.89 \pm 3.12\ cm^{-1}$, $\rho = 0.024 \pm 0.0017$, $\bar{\chi}_0 = 0.0014 \pm 5.67 \times 10^{-5}$ emu/octanuclear unit; $H = 1000$ G, $J = -160.98 \pm 11.66\ cm^{-1}$, $zJ' = +3.69 \pm 2.39\ cm^{-1}$, $\rho = 0.027 \pm 0.0015$, $\bar{\chi}_0 = 0.0013 \pm 5.53 \times 10^{-5}$ emu/octanuclear unit; $H = 10{,}000$ G, $J = -164.45 \pm 17.09\ cm^{-1}$, $zJ' = +7.88 \pm 4.12\ cm^{-1}$, $\rho = 0.024 \pm 0.0022$, $\bar{\chi}_0 = 0.0016 \pm 7.07 \times 10^{-5}$ emu/octanuclear unit. These parameters correspond to the theoretical curves shown as solid lines in Fig. 4.

The J values obtained here are also in concordance with a strong antiferromagnetic coupling between the unpaired electrons of the Cu(II) centers. The zJ' values allow us to suggest the existence of very weak interring magnetic coupling, although it could be suspected to be of a ferromagnetic type. The contribution of the noncoupled $S = 1/2$ spins in the sample (ρ in Eq. [1]) is lower than that found for [Cu(II) (μ-pz) (μ-OH)], in agreement with the previous discussion of the M–H plots for both compounds. The differences in such contributions stand out in the form of the $\bar{\chi}$–T curves in the low-temperature region for the two Cu(II) compounds studied here.

The significant contribution of non-coupled spins (noticeable at low temperatures as Curie-Weiss type behavior) affects the magnetic response of the studied compounds, for which, in addition, the $\bar{\chi}$ values are small. When fitting Eq. [1] to the experimental data, we noticed that the calculated temperature at which the molar magnetic susceptibility should be a maximum lies well below both that estimated experimentally and that predicted by the pure octanuclear model (Eq. [1] with $\rho = 0$) which is $T(\bar{\chi}_{max}) = |J|/k$ (16). Note that the last term in Eq. [1] shows the dependence of $\bar{\chi}$ on ρ and T. To study the effect of the mole fraction of noncoupled spins on the behavior of the molar magnetic susceptibility, we fitted Eq. [1] with $\rho = 0$ to the experimental data of both compounds at $H = 100$ G for the temperature range 50–300 K, and used the J and $\bar{\chi}_0$ values obtained in this way to theoretically calculate the

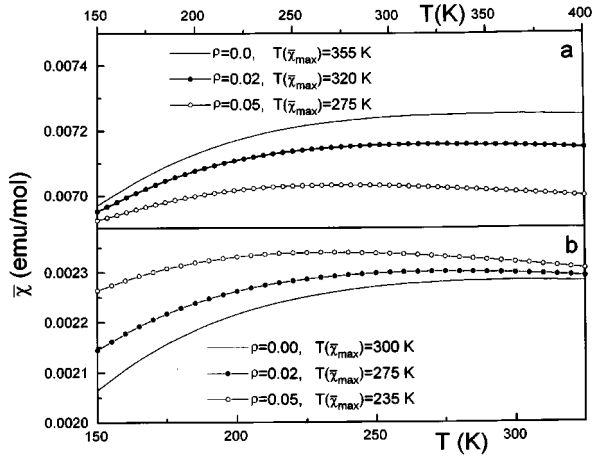

FIG. 5. $\bar{\chi}$(emu/mol)–T(K) theoretical curves from Eq. [1] for (a) [Cu(II)(μ-pz)(μ-OH)], and (b) [Cu(II)$_8$(μ-dmpz)$_8$(μ-OH)$_8$], as a function of the magnetic contribution of the noncoupled $S = 1/2$ spins.

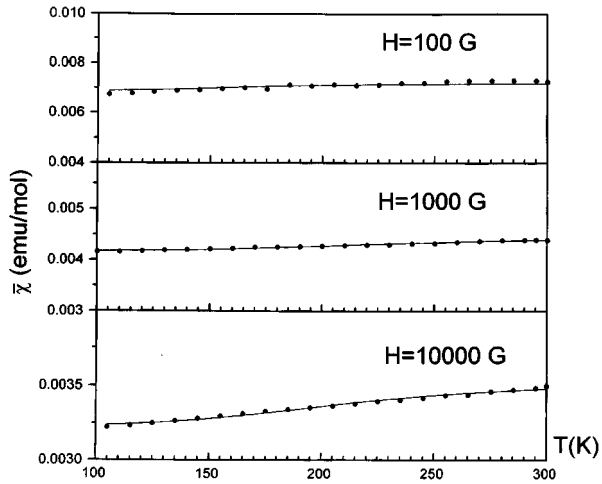

FIG. 6. $\bar{\chi}$(emu/mol)–T(K) values for [Cu(II)(μ-pz)(μ-OH)] and $H = 100$, 1000, and 10,000 G. Dotted lines are the experimental data and solid lines are theoretical values from Eq. [2].

molar magnetic susceptibility curves as a function of ρ with Eq. [1]. These are shown in Figure 5 for (a) [Cu(II)(μ-pz)(μ-OH)], and (b) [Cu(II)$_8$(μ-3,5-dmpz)$_8$(μ-OH)$_8$]. As can be seen, the temperature for which $\bar{\chi}$ has a maximum value is lower as ρ is increased. The presence of noncoupled spins, considered as a magnetic impurity, modifies the curve form and the $T(\bar{\chi}_{\max})$ values for both compounds.

In the next step, we proceeded to fit Eq. [1] with $\rho = 0$ to the experimental data for the 100–300 K temperature region, in which the effect of the magnetic impurity is not as noticeable as that in the low-temperature region. The magnetic results employing this pure octanuclear model are for [Cu(II)(μ-pz)(μ-OH)] with $g = 2.14$: $H = 100$ G, $J = -331.32 \pm 22.28\ \mathrm{cm}^{-1}$, $\bar{\chi}_0 = 0.0067 \pm 6.56 \times 10^{-5}$ emu/mol; $H = 1000$ G, $J = -363.50 \pm 5.19\ \mathrm{cm}^{-1}$, $\bar{\chi}_0 = 0.0041 \pm 5.52 \times 10^{-6}$ emu/mol; $H = 10{,}000$ G, $J = -346.64 \pm 5.20\ \mathrm{cm}^{-1}$, $\bar{\chi}_0 = 0.0032 \pm 6.30 \times 10^{-6}$ emu/mol; and for [Cu(II)$_8$(μ-3,5-dmpz)$_8$(μ-OH)$_8$] with $g = 2.20$: $H = 100$ G, $J = -231.23 \pm 35.77\ \mathrm{cm}^{-1}$, $\bar{\chi}_0 = 0.0018 \pm 1.09 \times 10^{-4}$ emu/mol; $H = 1000$ G, $J = -227.83 \pm 32.60\ \mathrm{cm}^{-1}$, $\bar{\chi}_0 = 0.0018 \pm 1.04 \times 10^{-4}$ emu/mol; $H = 10{,}000$ G, $J = -247.66 \pm 48.70\ \mathrm{cm}^{-1}$, $\bar{\chi}_0 = 0.0021 \pm 1.31 \times 10^{-4}$ emu/mol.

Although the fitting results are very good for both compounds and the three magnetic fields, the fact of reducing the number of experimental data make the statistical errors grow. Nevertheless, this procedure lets us see that the respective temperature for which $\bar{\chi}$ is a maximum ($|J|/k$) moves to a higher value than that calculated considering the contribution of noncoupled spins in the whole temperature range.

To analyze the possibility of interring interactions, we applied the octanuclear model with a mean-field correction (Eq. [2]) for the same range of temperatures (100–300 K) and $\rho = 0$. The fitting results were excellent, as can be seen in Fig. 6 for [Cu(II)(μ-pz)(μ-OH)] and Fig. 7 for [Cu(II)$_8$(μ-3,5-dmpz)$_8$(μ-OH)$_8$]. The magnetic parameters obtained are, for [Cu(II)(μ-pz)(μ-OH)] with $g = 2.14$ and $H = 100$ G, $J = -334.77 \pm 9.41\ \mathrm{cm}^{-1}$, $zJ' = -2.86 \pm 1.68\ \mathrm{cm}^{-1}$, $\bar{\chi}_0 = 0.0081 \pm 0.00089$ emu/mol; $H = 1000$ G, $J = -324.15 \pm 10.11\ \mathrm{cm}^{-1}$, $zJ' = -3.69 \pm 0.83\ \mathrm{cm}^{-1}$, $\bar{\chi}_0 = 0.0047 \pm 0.00014$ emu/mol; $H = 10{,}000$ G, $J = -311.67 \pm 9.18\ \mathrm{cm}^{-1}$, $zJ' = -4.05 \pm 0.92\ \mathrm{cm}^{-1}$, $\bar{\chi}_0 = 0.0036 \pm 0.00009$ emu/mol; for [Cu(II)$_8$(μ-3,5-dmpz)$_8$(μ-OH)$_8$] with $g = 2.20$ and $H = 100$ G, $J = -263.78 \pm 2.77\ \mathrm{cm}^{-1}$,

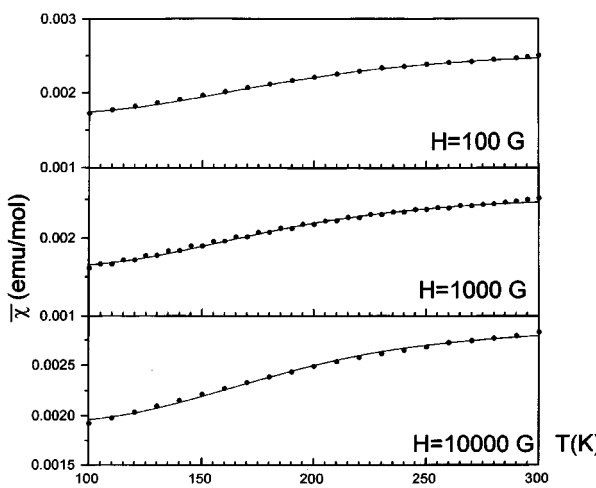

FIG. 7. $\bar{\chi}$(emu/mol)–T(K) values for [Cu(II)(μ-dmpz)$_8$(μ-OH)$_8$] and $H = 100$, 1000 and 10,000 G. Dotted lines are the experimental data and solid lines are theoretical values from Eq. [2].

$zJ' = 21.20 \pm 0.53\ cm^{-1}$, $\bar{\chi}_0 = 0.0013 \pm 8.88 \times 10^{-6}$ emu/mol; $H = 1000$ G, $J = -256.14 \pm 2.94\ cm^{-1}$, $zJ' = 25.33 \pm 0.59\ cm^{-1}$, $\bar{\chi}_0 = 0.0012 \pm 9.25 \times 10^{-6}$ emu/mol; $H = 10{,}000$ G, $J = -261.89 \pm 4.03\ cm^{-1}$, $zJ' = 24.06 \pm 0.75\ cm^{-1}$, $\bar{\chi}_0 = 0.0014 \pm 1.0 \times 10^{-5}$ emu/mol.

The pure octanuclear model with a mean-field correction also predicts higher temperature values for the $\bar{\chi}$ maximum for both Cu(II) compounds. The magnetic coupling parameter J for both compounds is in agreement with the above results about the proposition of strong antiferromagnetic coupling, slightly higher for [Cu(II)(μ-pz)(μ-OH)]. Also, this model and correction let us suggest the possibility of very weak interring magnetic coupling for both Cu(II) systems, maybe of antiferromagnetic type for [Cu(II)(μ-pz)(μ- OH)] and of ferromagnetic type for [Cu(II)$_8$(μ-3,5-dmpz)$_8$(μ-OH)$_8$]. Based on the spectral and magnetic studies, it is possible to suggest that the Cu(II) compound, with the unsubstituted pyrazolate ligand, shows an analogue structural arrangement to that of the cyclic octanuclear Cu(II) compound with the methylated pyrazolate ligand. The character (ferro- or antiferromagnetic) of the interring interactions zJ' is not conclusive, and at this point only the existence of this type of interactions can be suggested.

A very good fitting was also obtained applying the same cyclic octanuclear magnetic model and Eq. [1] with $\rho = 0$ to the magnetic data ($H = 100$ G) of the previously reported polynuclear compound [Cu(II)(allopurinolate)(OH)] (5), with $J = -378.23 \pm 19.0\ cm^{-1}$. The J value is of the same character as those corresponding to the Cu(II) compounds discussed here and also is in agreement with the structural arrangement suggested before for this Cu(II) system (5).

The dinuclear and the infinite linear chain magnetic models were employed in an attempt to explore the quality of the octanuclear ring magnetic model with respect to others in the description of the magnetic data presented here. The unsuccessful results in the fitting process for these two models lead us to conclude the reliability of the octanuclear ring model for the Cu(II) compounds discussed here.

When comparing the magnetic behavior of polynuclear bispyrazolate Cu(II) or Co(II) compounds (17–19) to that of the polynuclear system [Cu(II)(μ-pz)(μ-OH)], the former show lower superexchange magnetic coupling (J ranging from -6 to $-105\ cm^{-1}$). Dinuclear bispyrazolate Cu(II) compounds (20–22) show more intense magnetic coupling (J in the -100 to $-214\ cm^{-1}$ range). On the other hand, polynuclear bisdimethylpyrazolate Cu(II) or Co(II) compounds (11, 19, 23) (J in the -58 to $-66\ cm^{-1}$ range for Cu(II); from -2 to $-6.6\ cm^{-1}$ for Co(II)) also show lower magnetic coupling than [Cu(II)$_8$(μ-3,5-dmpz)$_8$(μ-OH)$_8$]. For dinuclear or trinuclear bispyrazolate Co(II) systems (24), the antiferromagnetic coupling is very low (J ranging from -1 to $-25\ cm^{-1}$).

The compound [Cu(II)(μ-pz)(μ-OH)] shows magnetic coupling in the same range as that shown by dinuclear Cu(II) compounds with pyrazolic and OR donor groups as bridges (25–28) (J from -32 to $> -500\ cm^{-1}$). With respect to the magnetic behavior of [Cu(II)(μ-3,5-dmpz)$_8$(μ-OH)$_8$], only one dinuclear case of this type was found in the literature (25). The magnetic coupling in this case is comparatively lower ($J = -95\ cm^{-1}$).

On the other hand, from all the dinuclear Cu(II) compounds quoted above (25–28), it is possible to analyze the influence of the methyl groups in the pyrazolic moiety on the magnetic coupling intensity of the respective systems. The only cases reported (25) (compounds quoted therein as 7a, J(pz/OR) $= -100\ cm^{-1}$; 7c, J(dmpz/OR) $= -95\ cm^{-1}$) show that the methyl groups do not have a strong influence on the intensity of the magnetic coupling. This influence is lower than that deduced from the magnetic study of the two Cu(II) compounds presented here.

CONCLUSIONS

In the present study, we performed the spectral and magnetic characterization of the polynuclear systems [Cu(II)(μ-pz)(μ-OH)] and [Cu(II)$_8$(μ-3,5-dmpz)$_8$(μ-OH)$_8$]. The spectral results allow us to suggest the pyrazolate and OH groups as mutually *trans* bridging ligands in the first system. This behavior is shown in [Cu(II)$_8$(μ-3,5-dmpz)$_8$(μ-OH)$_8$]. These systems are remarkable in their strong intraring superexchange magnetic coupling.

Finally, the Cu(II) compounds discussed before would be some of the few polynuclear Cu(II) systems which would have some topological relationship with the few octanuclear compounds reported up to now (29–32). They are also the first class of Cu(II) systems showing those mixed bridging ligands. This paper is the first magnetic study carried out for this type of very complex metallic systems.

ACKNOWLEDGMENTS

The authors are indebted to Francisco Morales-Leal (IIM, UNAM), Jorge Ramírez-Salcedo (IFC, UNAM), Carmen Vázquez (IIM, UNAM), and Leticia Baños (IIM, UNAM) for the magnetic susceptibility measurements, the EPR spectra, the TG measurements, and the X-ray diffraction patterns, respectively. We thank Maria Elena Solares and Milton Medeiros for throughly reading the manuscript. We also thank CONACyT (Grant 3170-E) for partial financial support. RE is indebted to OAS for financial support.

REFERENCES

1. J. Berthou, J. Elguero, and C. Rérat, *Acta Crystallogr. B* **26,** 1880 (1970).
2. J. A. S. Smith, B. Wehrle, F. A. Parrilla, H. H. Limbach, M. C. F. Foces, F. H. Cano, J. Elguero, A. Baldy, M. Pierrot, M. M. T. Khurshid, and J. B. L. McDouall, *J. Am. Chem. Soc.* **111,** 7304 (1989).
3. G. A. Ardizzoia, M. A. Angaroni, G. La Monica, F. Cariati, M. Moret, and N. Masciocchi, *J. Chem. Soc. Chem. Commun.* 1021 (1990).

4. G. A. Ardizzoia, M. A. Angaroni, G. La Monica, F. Cariati, S. Cenini, M. Moret, and N. Masciocchi, *Inorg. Chem.* **30,** 4347 (1991).
5. R. Acevedo-Chávez, M. E. Costas, and R. Escudero-Derat, *J. Solid State Chem.* **113,** 21 (1994).
6. M. K. Ehlert, S. J. Rettig, A. Storr, R. C. Thompson, and J. Trotter, *Can. J. Chem.* **68,** 1444 (1990).
7. J. Pons, X. López, E. Benet, J. Casabó, F. Teixidor, and F. J. Sánchez, *Polyhedron* **9,** 2839 (1990).
8. G. López, G. García, G. Sánchez, J. García, J. Ruíz, J. A. Hermoso, A. Vegas, and M. M. Ripoll, *Inorg. Chem.* **31,** 1518 (1992).
9. D. Carmona, J. Ferrer, I. M. Marzal, L. A. Oro, and S. Trofimenko, *Gazzetta Chim. Italiana* **124,** 35 (1994).
10. D. A. Johnson, A. W. Cordes, B. A. F. Kelley, and W. C. Deese, *J. Coord. Chem.* **32,** 1 (1994).
11. A. M. V. Sadus, *Transition Metal Chem.* **20,** 46 (1995).
12. J. Sletten, A. Sørensen, M. Julve, and Y. Journaux, *Inorg. Chem.* **29,** 5054 (1990).
13. M. Angaroni, G. A. Ardizzoia, T. Beringhelli, G. La Monica, D. Gatteschi, N. Masciocchi, and M. Moret, *J. Chem. Soc. Dalton Trans.* 3305 (1990).
14. G. López, J. Ruíz, G. García, C. Vicente, V. Rodríguez, G. Sánchez, J. A. Hermoso, and M. M. Ripoll, *J. Chem. Soc. Dalton Trans.* 1681 (1992).
15. D. Carmona, A. Mendoza, J. Ferrer, F. J. Lahoz, and L. A. Oro, *J. Organometallic Chem.* **431,** 87 (1992).
16. J. C. Bonner and M. E. Fisher, *Phys. Rev. A.* **135,** 640 (1964).
17. M. K. Ehlert, S. J. Rettig, A. Storr, R. C. Thompson, and J. Trotter, *Can. J. Chem.* **67,** 1970 (1989).
18. M. K. Ehlert, S. J. Rettig, A. Storr, R. C. Thompson, and J. Trotter, *Can. J. Chem.* **69,** 432 (1991).
19. M. K. Ehlert, A. Storr, and R. C. Thompson, *Can. J. Chem.* **71,** 1412 (1993).
20. T. Kamiusuki, H. Okawa, N. Matsumoto, and S. Kida, *J. Chem. Soc. Dalton Trans.* 195 (1990).
21. J. C. Bayon, P. Esteban, G. Net, P. G. Rasmussen, K. N. Baker, C. W. Hahn, and M. M. Gumz, *Inorg. Chem.* **30,** 2572 (1991).
22. J. Pons, X. López, J. Casabó, F. Teixidor, A. Caubet, J. Rius, and C. Miravitlles, *Inorg . Chim. Acta* **195,** 61 (1992).
23. M. K. Ehlert, A. Storr, and R. C. Thompson, *Can. J. Chem.* **70,** 1121 (1992).
24. M. K. Ehlert, S. J. Rettig, A. Storr, R. C. Thompson, and J. Trotter, *Can. J. Chem.* **71,** 1425 (1993).
25. W. Mazurek, B. J. Kennedy, K. S. Murray, M. J. O'Connor, J. R. Rodgers, M. R. Snow, A. G. Wedd, and P. R. Zwack, *Inorg. Chem.* **24,** 3258 (1985).
26. Y. Nishida and S. Kida, *Inorg. Chem.* **27,** 447 (1988).
27. T. N. Doman, D. E. Williams, J. F. Banks, R. M. Buchanan, H. R. Chang, R. J. Webb, and D. N. Hendrickson, *Inorg. Chem.* **29,** 1058 (1990).
28. M. K. Ehlert, S. J. Rettig, A. Storr, R. C. Thompson, and J. Trotter, *Can. J. Chem.* **70,** 2161 (1992).
29. J. Galy, A. Mosset, I. Grenthe, I. Puigdomènech, B. Sjöberg, and F. Hultén, *J. Am. Chem. Soc.* **109,** 380 (1987).
30. Q. Chen, S. Liu, and J. Zubieta, *Inorg. Chem.* **28,** 4433 (1989).
31. P. Gili, P. M. Zarza, G. M. Reyes, J. M. Arrieta, and G. Madariaga, *Polyhedron.* **11,** 115 (1992).
32. M. K. Ehlert, S. J. Rettig, R. C. Thompson, and J. Trotter, *Inorg. Chem.* **32,** 5176 (1993).